PCCP

Dynamic Article Links

Cite this: *Phys. Chem. Chem. Phys.*, 2012, **14**, 13746–13753

www.rsc.org/pccp

PERSPECTIVE

On the relationship between molecular state and single electron pictures in simple electrochemical junctions

Agostino Migliore,* Philip Schiff and Abraham Nitzan

Received 5th May 2012, Accepted 10th July 2012
DOI: 10.1039/c2cp41442b

We consider a molecular conduction junction that comprises a redox molecule bridging between metal electrodes, in the limit of weak coupling and high temperature where electron transport is dominated by Marcus electron transfer kinetics. We address the correspondence between the Marcus description in terms of nuclear potential energy surfaces associated with different charging states of the molecular bridge, and the single electron description commonly used in theories of molecular conduction. The relationship between the energy gap, reorganization energy and activation energy parameters of the Marcus theory and the corresponding energy parameters in the single electron description is elucidated. We point out that while transport in the normal Marcus regime involves activated (therefore relatively slow) transitions between at least two charging states of the molecular bridge, deep in the inverted regime only one of these states is locally stable and transitions into this state are activationless. The relatively slow rates that characterize the normal Marcus transport regime manifest themselves in the appearance of hysteresis in the system transport behavior as a function of gate or bias potentials for relatively slow scan rates of these potentials, but not bistability in the junction conduction behavior. We also consider the limit of fast solvent reorganization that may reflect the response of the electronic environment (electronic polarization of a solvent and of the metal electrodes) to the changing charging state of the bridge. In this limit, environmental reorganization appears as renormalization of the bridge electronic energy levels. We show that the effect of this reorganization on the junction conduction properties is not universal and depends on the particular bridge charging states that are involved in the conduction process.

School of Chemistry, Tel Aviv University, Tel Aviv, 69978, Israel.
E-mail: nitzan@post.tau.ac.il

Agostino Migliore

Agostino Migliore graduated in Physics from Palermo University in 2003. He earned a PhD in Physics in 2007 at the University of Modena and Reggio Emilia. After a post-doctoral position with Prof. Michael Klein at the University of Pennsylvania in 2007–2009, he joined Prof. Abraham Nitzan's group at Tel Aviv University, where he is currently a postdoctoral fellow. He is interested in electron transfer and molecular conduction junctions, with special attention to nonlinear charge transport phenomena such as negative differential resistance and hysteresis. He also collaborates with Dr Rosa Di Felice and other scientists on the investigation of modified DNAs.

Philip Schiff

Philip Schiff received a BS in Physics at Truman State University in 2004, and completed a PhD in Physics at Stony Brook University in 2009, where he studied transport in high temperature superconductors under the supervision of Adam Durst. He is a postdoc with Abraham Nitzan at Tel Aviv University where his research is focused on the influence of reorganization dynamics on transport properties of molecular materials and junctions.

1. Introduction

The Marcus theory of molecular electron transfer[1,2] and the Landauer theory of conduction in nanojunctions[3] were conceived within two years of each other. While each of them had decisive consequences on subsequent developments in the studies of electron transfer and transport, these important breakthroughs remained localized within different scientific communities for several decades. Indeed, extensive use of the Landauer theory in the context of molecular conduction junctions has started only in the 1990's,[4] and, while applications of the Marcus theory to electrode processes have increased gradually since Marcus first applied it in this context[5] (for comprehensive treatments see, *e.g.*, ref. 6 and 7), comprehensive studies of molecular conduction by Marcus-type kinetics, much of it by Ulstrup, Kuznetsov and coworkers, have started only in the late 1990's,[8–21] and explicit comparison between the theoretical contents of the Marcus and Landauer pictures was made only in the early 2000's.[22,23]

It is now well understood that the two mechanisms of electronic conduction belong to two extreme limits of transport phenomenology. The Landauer mechanism is a coherent co-tunneling process while the Marcus kinetics assumes subsequent metal–molecule and molecule–metal electron transfer processes with full reorganization of a polar solvent environment preceding each step. Obviously, intermediate situations should exist, and are indeed amply observed. First, particularly in weak molecule–electrode coupling situations and for near resonance tunneling, decoherence effects can convert the Landauer conduction into a subsequent hopping process even without prominent energetic effects. Second, an inelastic component in the tunneling current can be observed even when the dominant transport mechanism is still coherent. Stronger electron–vibration coupling can lead to richer and more intricate behavior, including non-linear effects such as current rectification, switching, negative differential conductance and hysteresis. For a review of inelastic effects on molecular conduction see ref. 24.

Abraham Nitzan

Abraham Nitzan is a professor of Chemistry and the director of the Sackler Institute of Advanced Studies at Tel Aviv University. His research focuses on theoretical aspects of chemical dynamics, in particular the interaction of light with molecular systems and charge transfer processes in condensed phases and interfaces. Among his main recognitions are the Humboldt Award, the ICS Prize and the Israel Prize in Chemistry. He is a Fellow of the American Physical Society and of the American Association for the Advancement of Science, a Foreign Honorary member of the American Academy of Arts and Sciences and a member of the Israel Academy of Arts and Sciences. In 2010 he has received an honorary doctorate (Dr Honoris Causa) from the University of Konstanz.

From the theoretical perspective, weak electron–vibrations coupling can be treated with relative ease, while processes involving stronger coupling pose substantial difficulties. Indeed, while some advances have been made,[25] we do not yet have a unified theoretical treatment that covers the full dynamic regime between the Landauer (no electron–vibration) and Marcus (subsequent hopping with full solvent reorganization coupling) limits.

Another difficulty encountered in addressing these limits stems from their different historical developments. The Landauer theory and subsequent theoretical treatments that include electron–vibration coupling are usually formulated in the representation of individual electrons interacting with individual vibrational modes, mostly using the harmonic approximation for the latter. The theory of molecular electron transfer, including electron transfer at molecule–electrode interfaces, is usually formulated in terms of molecular electronic states with the molecular nuclei moving on the corresponding Born–Oppenheimer surfaces (taken harmonic in line with the standard assumptions of linear dielectric solvent response and of harmonic intramolecular vibrations). A similar conceptual gap exists between standard theories of molecular spectroscopy and molecular junction transport.

Present efforts[26–30] to formulate non-equilibrium transport theory in terms of molecular states rather than single electron states, and other efforts to include many body correlation effects in the calculation of electron transport (see, *e.g.* ref. 31–33) are expected to eventually bridge this gap. In the present note we undertake the much simpler task of relating the conceptual pictures associated with the molecular and the single electron pictures to each other. While no new fundamental results are derived, this makes it possible to clarify some issues concerning the effect of solvent reorganization on the transport process.

2. Solvent reorganization in the single electron picture

Consider a junction comprising a molecule situated between two metal electrodes. The molecule will be represented by two electronic states that for definiteness we take to be the ground states of the neutral and negatively charged species, M and M^-, respectively. A polarizable environment responds to the molecular charge: in the Marcus framework this is described by the linear response of a continuum dielectric environment. Following Marcus, part of this response is assumed to be infinitely fast, while the other is slow relative to the electron dynamics. For simplicity, we discuss separately the slow and fast components of the environmental response. The effect of the latter is just to renormalize the electronic energy levels. In this section we assume that this has been taken into account (see Section 3) and focus on the slow solvent reorganization. In a homogeneous dielectric, this slow dielectric response is obtained using an effective dielectric constant $\varepsilon_{\mathrm{eff}} = \varepsilon_s\varepsilon_\infty/(\varepsilon_s - \varepsilon_\infty)$, where ε_s and ε_∞ are the total dielectric constant observed in a stationary field and its fast component associated with screening by the electronic motion, respectively. Several points should be made at the outset:

(a) The metal dielectric interface is obviously a non-homogeneous medium. Here the metal contributes a substantial part of the

fast response in the form of image interaction. The renormalization of molecular electronic energies by the fast dielectric response and the solvent reorganization energy associated with the slow dielectric response therefore depend on the molecule–metal(s) distance(s), molecular orientation and electrode(s) shape(s). In this note, which focuses on conceptual issues, we disregard these quantitative aspects, assuming that the solvent reorganization energy can be computed for any given junction configuration.

(b) It should be kept in mind that the assumption of time-scale separation, whereupon environmental response is partly much faster and partly much slower than the electron transfer dynamics, is an oversimplification of reality. Dynamical aspects of the environmental dielectric response should often be important. This is disregarded in the present discussion.

(c) In typical electrochemical setups, electrochemical gating is affected by a reference electrode that controls the potential difference between the working electrode and its molecular neighborhood. In the nano-size junction this potential difference is likely to be subjected to fluctuations associated with detailed motions of counterions inside the molecular junction. Such fluctuations are disregarded below as there are no indications that they are important on the characteristic time-scales of present experimental work. However it should be kept in mind that accounting for such fluctuations in the nano-environment of an electrochemical molecular junction may be required in future generalization of the present work.

(d) The following discussion focuses on processes that are dominated by Marcus kinetics. This implies that the molecule–electrode coupling is weak and that while the slow part of the solvent dielectric response is indeed slow relative to an electron hopping event, it is fast relative to the time between such events. Furthermore, broadening of molecular levels because of the molecule–metal coupling is disregarded. Consequently, the transitions $M \rightleftharpoons M^-$ are described by kinetic rates given by the Marcus electron transfer theory as applied to the metal–molecule interface. For each of the molecule–metal interfaces, characterized by electron transfer coupling V and metal Fermi energy E_F, these rates are given by

$$k_{M\to M^-} = \frac{1}{\sqrt{4\pi\lambda k_B T}}\int d\varepsilon \Gamma_1(\varepsilon) e^{-\frac{(\Delta E+\varepsilon-\lambda)^2}{4k_B T\lambda}} f(\varepsilon) \quad (1)$$

$$k_{M^-\to M} = \frac{1}{\sqrt{4\pi\lambda k_B T}}\int d\varepsilon \Gamma_1(\varepsilon) e^{-\frac{(\Delta E+\varepsilon+\lambda)^2}{4k_B T\lambda}} [1-f(\varepsilon)] \quad (2)$$

where

$$\Gamma_1(\varepsilon) = \frac{2\pi}{\hbar}\overline{|V_{1\varepsilon}|^2}\rho(\varepsilon) \quad (3)$$

is the golden rule rate for electron transfer between the "single electron level" 1 on the molecule (defined below) and single electron states of energy ε on the metal ($\overline{|V_{1\varepsilon}|^2}$ and $\rho(\varepsilon)$ are the corresponding average coupling and density of metal single electron states so that $\overline{|V_{1\varepsilon}|^2}\rho(\varepsilon) = \sum_k |V_{1k}|^2\delta(\varepsilon-\varepsilon_k)$) and

$$f(\varepsilon) = \frac{1}{e^{\varepsilon/(k_B T)}+1} \quad (4)$$

is the Fermi function. The single electron energies in the metal are calculated relative to the corresponding electrochemical potential μ. k_B and T are the Boltzmann constant and the temperature, respectively, and λ is the solvent reorganization energy.

Finally, ΔE is the energy difference

$$\Delta E = E_M(x_M) - E_{M^-}(x_{M^-}) + \mu, \quad (5)$$

where x_M and x_{M^-} represent the solvent configurations at equilibrium with the molecular species M and M^- and where μ is the electrochemical potential of electrons in the metal measured relative to vacuum, that is $\mu = -WF$ where WF is essentially the metal work function.[34] Note that $E_M(x_M) - E_{M^-}(x_{M^-})$ is the *adiabatic* ionization potential of the molecular negative ion, so ΔE is the energy difference between this quantity and the ionization potential of the metal. The integration over ε in eqn (1) and (2) reflects the fact that for a given electron transfer event the energy cost to remove an electron from the metal is $WF - \varepsilon$ and that the rates of electron removal and insertion are weighted by the population probability factors $f(\varepsilon)$ (that dominates for $\varepsilon < 0$) and $(1 - f(\varepsilon))$ (that dominates for $\varepsilon > 0$), respectively.

In the Marcus electron transfer theory the potential energy surfaces (in fact free energy surfaces), $E_M(x)$ and $E_{M^-}(x)$, are identical parabolas that are vertically and horizontally shifted with respect to each other. In the present context it is convenient to consider the surfaces $E_M(x)$ and $E_{M^-}(x) - \mu$ that are shown in Fig. 1 for several values of μ, *i.e.* different electrical potential drops between the molecule and the corresponding electrode.

A simple consideration can be used to estimate the energy differences between the M and M^- surfaces, provided that the energetics of solute–solvent interaction is assumed to be dominated by electrostatic/dielectric interactions. This assumption implies that the energy cost of moving a neutral solute from vacuum to solution can be disregarded. Consequently, the vertical energy difference between the M and M^- surfaces at the neutral solute configuration is determined by the energy

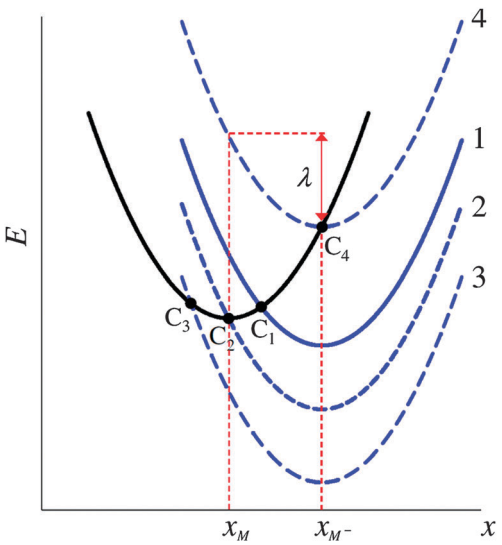

Fig. 1 Marcus parabolas, describing the system free energy as a function of the solvent dielectric coordinate, for the solute species M ($E_M(x)$, parabola centered about x_M, black) and M^-($E_{M^-}(x) - \mu$, parabola centered about x_{M^-}, blue). The latter is shown for different molecule–metal potential differences reflected in their vertical shift.

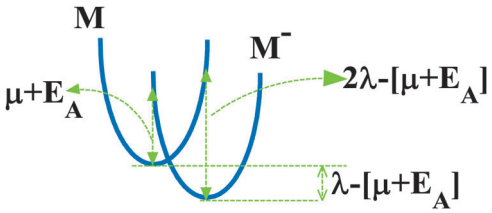

Fig. 2 Energy relationships between Marcus parabolas associated with the $M \rightleftharpoons M^-$ process, given in terms of the solvent reorganization energy (the Born solvation energy of the negative ion in the given dielectric environment), λ, the metal chemical potential (relative to vacuum) μ and the molecular electron affinity E_A.

needed to transfer an electron from the metal to the neutral molecule in vacuum, $\Delta E(\text{vac}) = E_M(\text{vac}) - E_{M^-}(\text{vac}) + \mu = E_M(x_M) - E_{M^-}(x_M) + \mu$. Note that the difference

$$E_A = E_M(\text{vac}) - E_{M^-}(\text{vac}) = E_M(x_M) - E_{M^-}(x_M) \quad (6)$$

is the vacuum ionization potential of the negative molecular ion, also known as the molecule electron affinity. This implies that the energy differences between the two Marcus parabolas relevant to our discussion are as shown in Fig. 2.

Next, consider the single electron picture of the conduction process, focusing for now on the zero bias limit. Fig. 3 shows the standard 1-electron picture that is used in elementary discussions of the application of Landauer theory to molecular conduction: a molecular single electron level between two electrodes characterized by their electrochemical potentials μ. In terms of the molecular states M and M^- the "single electron" energy expressed relative to μ is a function of the solvent reorganization coordinate x

$$\varepsilon_1(x) = E_{M^-}(x) - E_M(x) - \mu. \quad (7)$$

This linear function of x is represented by the red line in Fig. 3. It is important to note that in this composite picture, the solvation coordinate x is not in any way associated with the inter-electrode distance. It represents the evolution of the molecular single electron energy (relative to the metals Fermi energy) as solvation by solvent reorganization proceeds following an electron transfer state. Three points in these figures have particular significance: point $A \equiv (x_M, \varepsilon_1(x_M))$ represents the molecular single electron level when the solvent is in equilibrium with the neutral molecular species, point $B \equiv (x_{M^-}, \varepsilon_1(x_{M^-}))$ is the same level when the solvent is in equilibrium with the negative ion. In other words, in point A the solvent is in equilibrium with the unoccupied molecular level and in point B it is in equilibrium with the occupied one. The third significant point is $(x_c, \varepsilon_1(x_c) = 0)$ where the single electron energy is equal to the metal chemical potential. In the different cases displayed in Fig. 1 the latter are the points C_j ($j = 1,\ldots,4$) where the M and M^- parabolas cross.

Although the well-known kinetic rates (1) and (2) fully determine the Marcus dynamics, using the single electron picture of Fig. 3 can lead to new insight concerning electron transfer at molecule–electrode interfaces and electron transmission through junctions involving such interfaces:

(a) The Landauer theory describes transmission in the absence of solvent dynamics, that is, where the solvent configuration is frozen. If the solvent was frozen in the "neutral configuration" x_M,

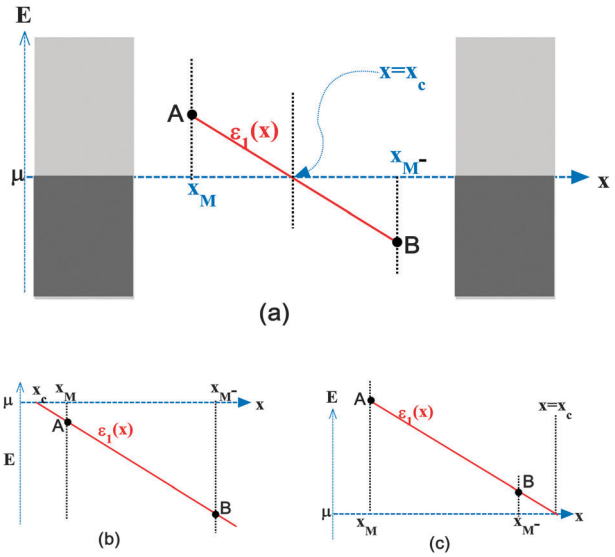

Fig. 3 A single electron picture of a junction (represented by a molecular single electron level coupled to two metal electrodes) controlled by Marcus kinetics. In (a), the electrodes are represented by the gray rectangles, with the darker gray representing filled single-electron levels. The coordinate x represents the environmental reorganization (including intramolecular nuclear motions) and is *not* related to the inter-electrode distance. $\varepsilon_1(x)$ is the linear function of x in the Marcus theory, and the segment shown connects between the point A, where the solvent is in equilibrium with the neutral molecule, and point B, where the solvent is in equilibrium with the molecular negative ion. The choice of the positive x direction as that associated with the $x_M \rightarrow x_{M^-}$ configuration change is arbitrary. The relationship $\varepsilon_1(x_M) > \varepsilon_1(x_{M^-})$ expresses the fact that it is energetically easier to charge the molecule when the solvent is in the configuration that minimizes the charging energy. Panel a corresponds to the normal Marcus regime (case 1 of Fig. 1) while panels b and c correspond to inverted Marcus regimes that are arrived through the points (C_2 and C_4 in Fig. 1, respectively) where the $M \rightarrow M^-$ and $M^- \rightarrow M$ processes became activationless.

electron transmission would involve an (often virtual) occupation of the single electron energy level $\varepsilon_1(x_M)$ represented by point A. Transmission through a frozen solvent configuration in equilibrium with the negative molecular ion corresponds to a hole transmission during which a hole in the otherwise occupied level $\varepsilon_1(x_{M^-})$ is transiently or virtually created. In Marcus kinetics, an electron transfer step does not take place in any of these configurations but, if the relevant metal energy is μ, at the point $(x_c, \varepsilon_1(x_c) = 0)$. Solvent fluctuation is needed to bring the system to this point starting from the equilibrium neutral or negative molecular species. Of course, other metal levels can be involved, which leads to the integral over ε in eqn (1) and (2) as discussed above.

(b) By applying an interfacial voltage V_g between molecule and electrode, the Fermi energy in Fig. 3a moves up or down, towards the situations depicted in Fig. 3b or c, respectively. At the voltage where the point A crosses the μ line (on the way to the situation of Fig. 3b), the Marcus parabolas (Fig. 1) cross at the minimum of the neutral molecule parabola (case 2, point C_2, of Fig. 1). At this point the rate $k_{M \rightarrow M^-}$ is activationless (with respect to a metal level at μ). Beyond this point we move into the Marcus inverted regime (case 3 of Fig. 1).

Similarly, the voltage where point B crosses the μ line corresponds to case 4 (point C_4) of Fig. 1, where the rate $k_{M^-\rightarrow M}$ is activationless with respect to metallic electron at μ, while beyond it, the situation described by Fig. 3c corresponds to the inverted regime (not shown in Fig. 1) reached beyond this point.

(c) In the application of Marcus theory to molecular electron transfer, the dependence of the transfer rate on the energy gap parameter, ΔE (eqn (5)), is characterized by a minimum (zero) in the activation energy of the corresponding rate as the system evolves from the normal to the inverted Marcus regime (point C_2 in Fig. 1 for $k_{M\rightarrow M^-}$ and point C_4 in the same figure for $k_{M^-\rightarrow M}$). Once in the inverted regime these rates are again affected by the need to surpass a nuclear barrier. For electrode processes the situation is different. Consider for example the process $M \rightarrow M^-$ in the case described by Fig. 3b. The stable nuclear configuration in the initial neutral state is x_M (point A in Fig. 3b). To get a metal electron of energy $\varepsilon = \mu$ requires a configurational fluctuation to x_c, so such a process would have been activated if the only available electrons were of this energy. However, since metal electrons of energy $\varepsilon_1(x_M)$ are available, the process remains activationless. The same is true for the process $M^- \rightarrow M$ in the situation represented by Fig. 3c. The Marcus inverted regimes can be formally defined, as done above, by referring to metal electrons of energy $\varepsilon = \mu$, but they lose their significance for electrode processes.

As functions of the interfacial potential V, the kinetics of the rate process $M \underset{k_{M^-\rightarrow M}}{\overset{k_{M\rightarrow M^-}}{\rightleftharpoons}} M^-$ (considered for a single molecule–metal interface or for a symmetric unbiased junction under a gate potential V_g) can be broadly described as falling into three regimes: between the two thresholds defined by

$$\Delta E(V_g) - \lambda = 0, \quad \Delta E(V_g) + \lambda = 0 \qquad (8)$$

(ΔE is given by eqn (5) in which $\mu = \mu(V_g = 0) + eV_g$ where e is the absolute value of the electron charge) both $k_{M\rightarrow M^-}$ and $k_{M^-\rightarrow M}$ are determined by activation barriers that depend on the reorganization energy.[35] These activation free energies determine the probabilities for fluctuations in the environmental configuration x from its stable positions x_M or x_{M^-}, respectively, to the configuration x_c where $\varepsilon_1(x_c) = 0$ when measured relative to μ. From eqn (5) and (8)

$$V_{g1} = \frac{1}{e}(E_{M^-}(x_{M^-}) - E_M(x_M) - \mu_0 + \lambda) \qquad (9a)$$

$$V_{g2} = \frac{1}{e}(E_{M^-}(x_{M^-}) - E_M(x_M) - \mu_0 - \lambda) \qquad (9b)$$

For $V_g > V_{g1}$ the process $M \rightarrow M^-$ behaves as essentially activationless while for $V_g < V_{g2}$ it is the $M^- \rightarrow M$ process that behaves in this way (see below for more rigorous statements). The corresponding opposite processes ($M^- \rightarrow M$ for $V_g > V_{g1}$ and $M \rightarrow M^-$ for $V_g < V_{g2}$) are inhibited by large ($>\lambda$) activation free energies. In this sense we can say the metal–molecule system is bistable for $V_{g2} < V_g < V_{g1}$, while only one state, either M or M^- is stable outside this potential range. This is seen in Fig. 4–6, which show these rates and the corresponding activation energy. The individual rates $k_{M\rightarrow M^-}$ and $k_{M^-\rightarrow M}$ (in units of Γ) are shown in Fig. 4, while Fig. 5 shows their sum, $R = k_{M\rightarrow M^-} + k_{M^-\rightarrow M}$, that determines the relaxation rate of this electron transfer system to equilibrium. Fig. 5 displays the activation energy $E_{act}/k_BT \equiv T\partial \ln(R)/\partial T$. Note that while the trends discussed above are clearly seen, because the metal provides or takes electrons at a range of energies, expressed by the ε integrations in eqn (1) and (2),

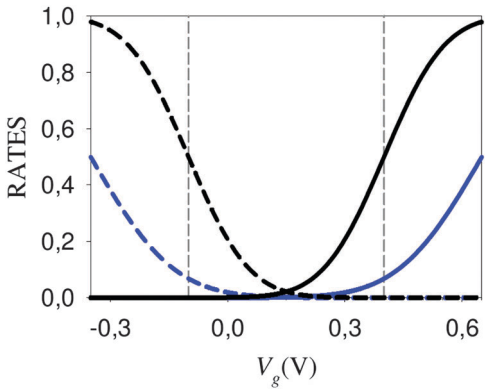

Fig. 4 $k_{M\rightarrow M^-}/\Gamma$ (solid line) and $k_{M^-\rightarrow M}/\Gamma$ (dashed lines), eqn (1) and (2), plotted against V_g. The reorganization energy λ is 0.25 eV (black lines) or 0.5 eV (blue lines). Other parameters are $E_{M^-}(x_{M^-}) - E_M(x_M) - \mu_0 = 0.15$ eV and $T = 298$ K. The vertical dashed lines mark the threshold values of V_g for $k_{M\rightarrow M^-}$ and $k_{M^-\rightarrow M}$, $V_{g1} = 0.4$ V and $V_{g2} = -0.1$ V for our choice of parameters with $\lambda = 0.25$ eV. The threshold values for $\lambda = 0.50$ eV are $V_{g1} = 0.65$ V, $V_{g2} = -0.35$ V, marked by the edges of the voltage axis.

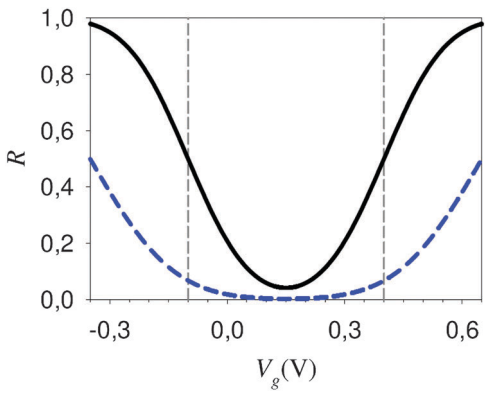

Fig. 5 The sum $R = (k_{M\rightarrow M^-} + k_{M^-\rightarrow M})/\Gamma$ plotted against V_g for $\lambda = 0.25$ eV (black full line) and $\lambda = 0.50$ eV (blue dashed line).

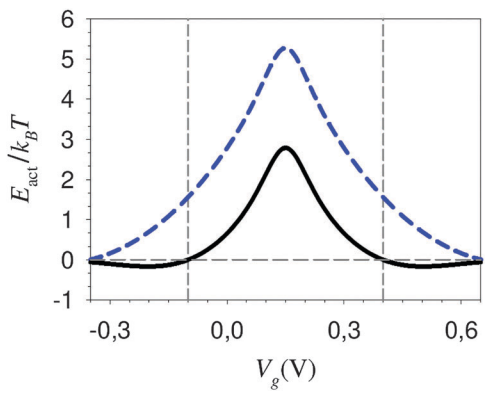

Fig. 6 The activation energy associated with the total relaxation rate R. Line notation is the same as in Fig. 5.

the threshold values V_{g1}, V_{g2} do not mark the exact rates saturation and vanishing of the activation energy. In fact, it can be shown[36] that at the threshold V_{g1} the rate $k_{M\rightarrow}M^-$ becomes $k_{M\rightarrow M^-} = (1/2)k^{max}_{M\rightarrow M^-}$, where $k^{max}_{M\rightarrow M^-}$ is the maximum rate obtained at the high voltage plateau. The same is true for the rate $k_{M^-\rightarrow M}$ at the threshold voltage V_{g2}.

The bistable nature of the system, manifestly expressed between the voltage thresholds, will translate into its behavior in a cyclic voltammetry measurement in which the system state is monitored while V_g changes cyclically. The observed response, in particular the possible appearance of hysteresis, reflects timescales in the system in comparison to timescale associated with the voltage change. Obviously, hysteresis will appear in the range between V_{g1} and V_{g2} for voltage change rates much smaller than those needed to observe it outside this range.

Bistability is also an important attribute in the conduction response of molecular junctions. It is important to realize that the bistable nature of the molecule–electrode electron transfer system, as described above, cannot translate, within the model considered, into conduction bistability. The reason for this is that a single channel conduction governed by Marcus kinetics is determined by an electron transmission process that involves both charging and de-charging of the bridging molecular redox species. Indeed, the zero bias conductance is easily shown to be given by

$$G(0) = \frac{e^2}{k_B T}\frac{k^L_{M\rightarrow M^-}(0)k^R_{M^-\rightarrow M}(0)}{k^L_{M\rightarrow M^-}(0) + k^R_{M\rightarrow M^-}(0) + k^L_{M^-\rightarrow M}(0) + k^R_{M^-\rightarrow M}(0)} \quad (10)$$

where the superscripts L and R correspond to the left and right electrodes, (0) indicates that all rates are evaluated at zero bias voltage and where symmetry is satisfied because[36] $k^L_{M\rightarrow M^-}(0)k^R_{M^-\rightarrow M}(0) = k^R_{M\rightarrow M^-}(0)k^L_{M^-\rightarrow M}(0)$. Fig. 7 shows that in fact $G(0)$ goes through a maximum within the $V_{g2} < V_g < V_{g1}$ region (marked by the vertical dashed lines). This behavior mostly reflect dependence of $G(0)$ on the product of Fermi functions $f_R(1 - f_L) = f_L(1 - f_R)$, which maximizes near the Fermi energy.

We conclude this section with some comments. First, in the above analysis we have addressed the common situation where Marcus kinetics governs the electron transfer between the molecule and both electrodes. It is in principle possible, in strongly asymmetric junctions, that electron transfer between the molecule and one electrode will be controlled by Marcus kinetics while transfer to/from the other electrode will occur *via* instantaneous tunneling. We do not know any such systems, and expect such occurrences to be rare because Marcus kinetics appears in cases of weak molecule–electrode coupling that result from the localized nature of the relevant molecular orbital. However, this localization usually renders weak molecule–electrode coupling and consequently Marcus-type kinetics at both molecule–electrode interfaces.

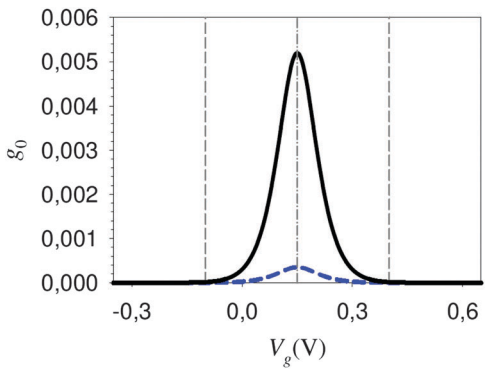

Fig. 7 $g_0 \equiv \frac{k_B T}{e^2} G(0)$, plotted against V_g for a symmetric junction in which the molecule–electrode kinetics is determined by the same rate parameters as in Fig. 4–6. Line notation is as in Fig. 5 and 6.

Second, while the above analysis of electron transfer and transmission at molecule–electrode interface(s) was done in terms of the molecular process $M \rightleftharpoons M^-$, it should be clear that the same analysis applies where M is replaced by "oxidized species" and M^- by "reduced species".

Finally, as noted above, the bistable nature of the molecular charging state for $V_{g2} < V_g < V_{g1}$ does not translate into multiple conduction states because the conduction process involves repeated transitions between the oxidized and reduced forms of the molecule. (We note in passing that in the same junction model in the strong molecule–lead coupling limit, the *adiabatic* potential surface for the nuclear configuration can assume multiple minima that correspond to different conduction states of the junction.[37]). However, switching between charging states can translate into switching between electron transport behavior if electron transmission is dominated by a different conduction channel in a way that depends on the molecule charging state. We will elaborate on this issue elsewhere.[38]

3. The effect of fast environmental response

The discussion in Section 2 has focused on the effect of solvent reorganization that takes place on a timescale long relative to electron transfer events and fast relative to the time between such events. Such slow response characterizes molecular nuclear motions as well as the nuclear component of solvent dielectric response. Here we focus on the fast (electronic) component of the environmental response, limiting ourselves to the assumption that this response is much faster than electron hopping events relevant to the observed conduction. Under this assumption the fast environmental response just amounts to renormalization of the molecular electronic energies.

How does such renormalization affect conduction? In a recent paper,[33] Wang and coworkers have considered the effect of electron–nuclear vibrations coupling on the electronic transport behavior of the standard junction model comprising a single electronic level bridge coupled to two free electron reservoirs and to vibrational modes:

$$\hat{H} = \hat{H}_{el} + \hat{H}_{nuc} + H_{el\text{-}nuc} \quad (11)$$

$$\hat{H}_{el} = \varepsilon_l \hat{c}^\dagger_l \hat{c}_l + \sum_l \varepsilon_l \hat{c}^\dagger_l \hat{c}_l + \sum_r \varepsilon_r \hat{c}^\dagger_r \hat{c}_r + \sum_l (V_{ll}\hat{c}^\dagger_l \hat{c}_l + V_{ll}\hat{c}^\dagger_l \hat{c}_l) + \sum_r (V_{lr}\hat{c}^\dagger_l \hat{c}_r + V_{rl}\hat{c}^\dagger_r \hat{c}_l) \quad (12)$$

$$\hat{H}_{nuc} = (1/2)\sum_j (\hat{P}^2_j + \omega^2_j \hat{Q}^2_j) \quad (13)$$

$$\hat{H}_{el\text{-}nuc} = \hat{c}^\dagger_l \hat{c}_l \sum_j c_j \hat{Q}_j \quad (14)$$

where $\hat{c}$, $\hat{c}^{\dagger}$ denote annihilation and creation operators for electrons, subscripts 1, l and r correspond to the molecular state and to states of the left and right electrodes, respectively, $\hat{P}_j$, $\hat{Q}_j$ are momentum and position operators for the j-th harmonic nuclear mode and the coefficients c_j represent the electron–nuclear coupling on the molecular species. Specifically, they consider a continuum of vibrational modes with an Ohmic spectral density

$$J(\omega) \equiv \frac{\pi}{2}\sum_j \frac{c_j^2}{\omega_j}\delta(\omega-\omega_j) = \frac{\pi}{2}\alpha\omega e^{-\omega/\omega_c}, \qquad (15)$$

characterized by the cutoff frequency ω_c and the dimensionless Kondo parameter α, for which the reorganization energy is given by $\lambda = 2\alpha\omega_c$, however the following observation (Fig. 3 and 4 of ref. 33) is generic: when λ increases from zero, the current obtained by applying a small bias potential between the electrodes increases in the case where ε_1 is larger than the electrochemical potentials μ_L,μ_R of both leads (electron transport) and decreases in the opposite case, where $\varepsilon_1 < \mu_L$,μ_R (hole transport). This observation is rationalized by the downward polaron shift (solvation in the harmonic environment) of the molecular level, which puts the level closer to μ_L,μ_R the first case, thus enhancing transmission, and further away from μ_L,μ_R in the second, thus making transmission less efficient.

We have verified these results using a simple one nuclear oscillator model. Furthermore, the interpretation in terms of the polaron shift becomes rigorous in the fast solvent reorganization limit. In this limit the solvation coordinate x becomes irrelevant. The molecular single electron energy to be used, for a transport dominated by the $M \rightleftharpoons M^-$ electron exchange process, is the number $\varepsilon_1 = E_{M^-}(x_{M^-}) - E_M(x_M) - \mu$. When $\varepsilon_1 > 0$ we have an electron transport mechanism while $\varepsilon_1 < 0$ corresponds to a hole transport process. The observation described above amounts to the statement that when the solvent reorganization energy (stabilization of M^-) is larger, the energy cost of putting an excess electron on M decreases, while that of removing an electron from M^- increases. More generally, if N is the number of electrons on the molecule, "electron transport" *via* the process $N \rightarrow N+1 \rightarrow N$ becomes easier, while hole transport, $N+1 \rightarrow N \rightarrow N+1$, becomes more difficult if increasing solvent polarization stabilizes the $N+1$ species. Of course the charging state may be such that the solvent stabilizes the N form relative to the $N+1$ form, in which case its effect is reversed, enhancing the hole transport process and inhibiting the electron transport one.

However, while this statement is obviously correct, its implications should be regarded with caution. In general one refers to electron and hole transport processes with regards to the highest occupied molecular orbital, HOMO, and the lowest unoccupied molecular orbital, LUMO, of a molecule bridging between two metal leads. If the molecule contains N electrons at equilibrium, "electron transport" *via* the LUMO is the process $N \rightarrow N+1 \rightarrow N$, while hole transport *via* the HOMO is described by $N \rightarrow N-1 \rightarrow N$. In this picture solvent reorganization can affect electron and hole conduction in the same way. Suppose, for example, that the N-electron molecule is neutral. Fast solvation of the charged $N+1$ or $N-1$ ions makes it easier both to add and to remove an electron from this molecule. However, two caveats should be noted. First, for a real structured solvent, the solvation energy of positive and negative ions is not generally the same, so the solvent effect on transport *via* the LUMO and HOMO orbitals will be quantitatively different. Second, the actual observation depends on the particular charging state of the equilibrium junction: if in the last example the N electron molecule is positively charged, the $N \rightarrow N+1 \rightarrow N$ processes may be enhanced while the $N \rightarrow N-1 \rightarrow N$ may be inhibited by the solvent induced renormalization of the $N/N+1$ and $N/N-1$ energy gaps.

4. Summary

Junction transport by Marcus kinetics is an essentially solved problem. Here we have considered this process from a new perspective that has provided some new insights:

(a) In a single electron picture of this process, the molecular single electron level, here denoted ε_1, is a linear function of the solvation coordinate, $\varepsilon_1(x)$. Three points on this line are particularly significant: for a transfer process associated with the $M \rightleftharpoons M^-$ molecular transitions these are $\varepsilon_1(x_M)$, $\varepsilon_1(x_{M^-})$ and $\varepsilon_1(x_c)$. x_M and x_{M^-} correspond to the minima of the Marcus parabolas associated with the M and M^- species, while x_c is the point where these parabolas cross. In an equilibrium junction $\varepsilon_1(x_c) = \mu$ where μ is the electrochemical potential characterizing the leads. In the normal Marcus regime $\varepsilon_1(x_M)$, $\varepsilon_1(x_{M^-})$ are positioned on the two sides of μ (*i.e.* one is larger and one is smaller than μ). Inverted Marcus regimes correspond to $\varepsilon_1(x_M)$, $\varepsilon_1(x_{M^-})$ both larger or both smaller than μ.

(b) In the normal Marcus regime the M and M^- (in the particular example discussed; more generally we could consider molecular species with N, $N+1$ electrons) are (as usual in the Marcus theory) locally stable, where the free energy barrier between them is determined by the molecular electronic structure and the solvent reorganization energy. Unlike in the Marcus theory for molecular electron transfer, deep in the inverted regime only one of the charging states is stable, and transition into this state is activationless.

(c) The bistable nature of the molecular charging states in the Marcus normal regime is not associated with bistability in the conduction of this junction model, but implies, as usual, hysteresis in cyclic voltage bias scans with relatively small speeds.

These observations are made within the standard Marcus approach that assumes that solvent response is in part much faster, and in part much slower, than the relevant electron dynamics, and are associated with the slow part of the solvent reorganization. The fast solvent response affects only renormalization of molecular electronic energies. We have considered also this effect and concluded that implications of recent observations of the effect of solvent reorganization on electron and hole transfer transport mechanisms be analyzed with caution. Predictions of specific effects of this kind can be made only in conjunction with the charging states of the molecular bridge that are involved in the electron transmission process.

Acknowledgements

We thank M. Galperin for many helpful discussions and for technical help. This work was supported by the

Israel Science Foundation, the European Research Council under the European Union's Seventh Framework Program (FP7/2007–2013; ERC grant agreement no 226628) and the Israel Niedersachsen Research Fund.

References

1 R. A. Marcus, *J. Chem. Phys*., 1956, **24**, 966.
2 R. A. Marcus, *J. Chem. Phys*., 1956, **24**, 979.
3 R. Landauer, *IBM J. Res. Dev*., 1957, **1**, 223.
4 For a review see:A. Nitzan, *Annu. Rev. Phys. Chem*., 2001, **52**, 681–750.
5 R. A. Marcus, *Electrochim. Acta*, 1968, **13**, 995–1004.
6 W. Schmickler, *Interfacial Electrochemistry*, Oxford University Press, Oxford, 1996.
7 A. Nitzan, *Chemical Dynamics in Condensed Phases*, Oxford Univ. Press, Oxford, 2006, ch. 17.
8 E. P. Friis, Y. I. Kharkats, A. M. Kuznetsov and J. Ulstrup, *J. Phys. Chem. A*, 1998, **102**, 7851–7859.
9 A. M. Kuznetsov and J. Ulstrup, *J. Phys. Chem. A*, 2000, **104**, 11531–11540.
10 A. M. Kuznetsov and J. Ulstrup, *J. Chem. Phys*., 2002, **116**, 2149–2165.
11 J. Zhang, A. M. Kuznetsov and J. Ulstrup, *J. Electroanal. Chem*., 2003, **541**, 133–146.
12 A. M. Kuznetsov, I. G. Medvedev and V. V. Sokolov, *J. Chem. Phys*., 2004, **120**, 7616–7635.
13 A. M. Kuznetsov and J. Ulstrup, *J. Electroanal. Chem*., 2004, **564**, 209–222.
14 A. A. Kornyshev, A. M. Kuznetsov and J. Ulstrup, *ChemPhysChem*, 2005, **6**, 583–586.
15 A. A. Kornyshev, A. M. Kuznetsov and J. Ulstrup, *Proc. Natl. Acad. Sci. U. S. A*., 2006, **103**, 6799–6804.
16 W. Haiss, T. Albrecht, H. vanZalinge, S. J. Higgins, D. Bethell, H. Hobenreich, D. J. Schiffrin, R. J. Nichols, A. M. Kuznetsov, J. Zhang, Q. Chi and J. Ulstrup, *J. Phys. Chem. B*, 2007, **111**, 6703–6712.
17 A. M. Kuznetsov, *J. Chem. Phys*., 2007, **127**, 084710.
18 A. A. Kornyshev and A. M. Kuznetsov, *J. Phys.: Condens. Matter*, 2008, **20**, 374103.
19 A. M. Kuznetsov, I. G. Medvedev and J. Ulstrup, *J. Chem. Phys*., 2009, **131**, 16.
20 A. M. Kuznetsov, I. G. Medvedev and J. Ulstrup, *J. Chem. Phys*., 2009, **131**, 164703–164716.
21 For a review see:J. D. Zhang, A. M. Kuznetsov, I. G. Medvedev, Q. J. Chi, T. Albrecht, P. S. Jensen and J. Ulstrup, *Chem. Rev*., 2008, **108**, 2737–2791.
22 A. Nitzan, *J. Phys. Chem. A*, 2001, **105**, 2677–2679.
23 A. Nitzan, *Isr. J. Chem*., 2002, **42**, 163–166.
24 M. Galperin, M. A. Ratner and A. Nitzan, *J. Phys.: Condens. Matter*, 2007, **19**, 103201.
25 See, *e.g*.S. Yeganeh, M. A. Ratner and V. Mujica, *J. Chem. Phys*., 2007, **126**, 161103.
26 M. Galperin, A. Nitzan and M. A. Ratner, *Phys. Rev. B: Condens. Matter Mater. Phys*., 2008, **78**, 125320–125329.
27 S. Yeganeh, M. A. Ratner, M. Galperin and A. Nitzan, *Nano Lett*., 2009, **9**, 1770–1774.
28 M. Esposito and M. Galperin, *Phys. Rev. B: Condens. Matter Mater. Phys*., 2009, **79**, 205303–205312.
29 M. Esposito and M. Galperin, *J. Phys. Chem. C*, 2010, **114**, 20362–20369.
30 A. J. White and M. Galperin, this issue.
31 U. Harbola and S. Mukamel, *Phys. Rep*., 2008, **465**, 191–222.
32 A. A. Dzhioev and D. S. Kosov, *J. Chem. Phys*., 2011, **134**, 154107.
33 H. Wang, I. Pshenichnyuk, R. Hartle and M. Thoss, *J. Chem. Phys*., 2011, **135**, 244506–244513.
34 By ''essentially'' we refer to the difference between the thermodynamic electrochemical potential and the practical definition of the workfunction. The latter refers to removing an electron from the metal to just outside it, while WF $= -\mu$ is the work needed to remove an electron from the metal to vacuum at infinity.
35 In this range of V_g the crossing point of the two parabola lies between points C2 and C4 of Fig. 1. The larger of the two activation free energies is at most equal to λ.
36 A. Migliore and A. Nitzan, *ACS Nano*, 2011, **5**, 6669–6685.
37 M. Galperin, M. A. Ratner and A. Nitzan, *Nano Lett*., 2004, **5**, 125–130.
38 A. Migliore and A. Nitzan, to be published.